Co-evolution of Sensory System and Signal Processing for Optimal Wing Shape Control

Olga Smalikho[1(✉)] and Markus Olhofer[2]

[1] Technische Universität Darmstadt, Darmstadt, Germany
Olga.Smalikho@rtr.tu-darmstadt.de
[2] Honda Research Institute Europe, Offenbach, Germany
Markus.Olhofer@honda-ri.de

Abstract. This paper demonstrates the applicability of evolutionary computation methods to co-evolve a sensor morphology and a suitable control structure to optimally adjust a virtual adaptive wing structure. In contrast to approaches in which the structure of a sensor configuration is fixed early in the design stages, we target the simultaneous generation of information acquisition and information processing based on the optimization of a target function. We consider two aspects as main advantages. First the ability to generate optimal environmental sensors in the sense that the control structure can optimally utilize the information provided and secondly the abdication of detailed prior knowledge about the problem at hand. In this work we investigate the expected high correlation between the sensor morphology and the signal processing structures as well the quantity and quality of the information gathered from the environment.

Keywords: Co-evolution · Neural network · Robust optimization

1 Introduction

Adaptive systems consist of sensors as well as actuators which allow the improvement of systems in reaction to changes in their environment according to a predefined quality measure. The design of such systems is usually driven by the utilization of prior knowledge of the problem at hand in order to generate an effective sensory system which is able to provide all relevant information about the environmental conditions as well as actuator configurations which can generate suitable reactions to improve the system's performance. After the determination of the sensor and actuator configuration a suitable control structure which processes information from the environment to effective actuator signals is generated. This procedure requires a detailed understanding of all phenomena which influence the behavior of the system. One reason is the necessity of knowing what information about the environment is important in order to place the right sensors at the right place. To acquire this knowledge a priori is challenging for a wide variety of tasks. Furthermore, the determination of an optimal overall system is expected to be challenging due to strong interaction between the

A.I. Esparcia-Alcázar et al. (Eds.): EvoApplications 2014, LNCS 8602, pp. 805–816, 2014.
DOI: 10.1007/978-3-662-45523-4_65

sensor and actuator configuration with the control system. Therefore it is necessary to solve two tasks. The first is to determine the optimal control structure for the provided information by sensors, and secondly to determine information which optimally suits the control system. In this research we demonstrate the simultaneous evolutionary design of sensor configuration and control structure for the example of a virtual adaptive wing configuration. Based on the evolved designs we investigate the influence of the sensory input dimensionality on the overall system quality. In detail we analyze the trade off between more detailed information which requires the generation of a more complex information processing system and a low dimensional sensory input which is able to acquire a reduced set of environmental information, however requiring a simpler and easier to generate control structure. We demonstrate that both factors are in a trade off relation. Furthermore we invest the co-evolution process of both units and demonstrate the high dependency between sensor and control structure. A variety of similar approaches for the evolutionary design of sensor and actuator configurations have been investigated in the field of evolutionary robotics. Early work in the field of automatic design of a systems by body-brain co-evolution has been reported by Sims [1]. He demonstrated the evolutionary development of the morphology of virtual creatures in a physical simulation fulfilling simple locomotion tasks starting from simple building blocks without any prior knowledge. Parker and Nathan [2] research the design of sensor morphology and controller for a simulated hexapod robot. For this purpose the type of sensors, the heading angle and the range of the sensors as well as the rules for the controller are co-evolved. This method enables the system to extract information from the environment which is relevant to complete a given task by configuring a minimal controller and number of sensors to increase the system's overall efficiency. Bugajska and Schutz [3] co-evolved the shape and strategies in the design of Micro Air Vehicles (MAV). The target, similar to Parker and Nathan, was to find a minimal sensor suite and reactive strategies for navigation and collision avoidance tasks. Sugiura et al. also proposed a system that automatically designs the sensor morphology of an autonomous robot with two kinds of adaptation: ontogenetic and phylo-genetic adaptation[4]. Also Auerbach and Bongard [5] have made extensive research in the field of co-evolution of morphology and control in evolutionary robotics. In their work they implement a growth mechanism to create robots using compositional pattern-producing networks and demonstrate that the concurrent development of the morphological and controller structures of the simulated adaptive robots can give an advantage for the final system performance, compared to the approaches with separate design strategies.

Compared with the reviewed research in evolutionary robotics, we utilize the co-evolution of morphology and information processing structure for the optimal control of an adaptive wing shape. Although the generation of optimal control for adaptive wings is not in the main focus of our research we argue that this problem is a suitable test bed for the research on evolutionary design of adaptive systems. Aerodynamic problems are characterized by highly complex interactions between flow body and flow field which is in most cases difficult to understand

in detail. Due to this manual design is generally challenging to achieve. However excellent tools are available for their simulation and the evaluation. In this work we demonstrate that evolutionary methods are able to generate systems which can optimally adapt to environmental conditions, while at the same time we target shedding some light on the precise synchronization of system parts during the developmental process. In comparison to the research [2],[3],[4] we changed the environmental settings randomly in each generation of the evolutionary process and thus obtained a robust adaptive system, able to react during random environmental changes. The target for the development of the adaptive wing is the reduction of the drag the airfoil generates while still creating a minimum of lift. Environmental changes are realized by changes in the angle of attack of the airflow across a wide range. A detailed description of the adaptive wing and the experimental conditions is given in section 2. In section 3 we summarize results of standard design optimization tasks for non-adaptive airfoils in order to generate a baseline for the comparison of the quality achieved by the adaptive system. An airfoil design optimization for a certain number of the fixed environmental conditions, represented in section 3, shows maximal controller potentials for these environmental conditions. In Section 4 we describe the experiments we performed, present results of the experiments and analyze the development process realized. Finally we conclude the paper by a summary of the main findings and an outlook of further work.

2 Framework for Morphology-Controller Co-evolution

In our work we implemented a system, consisting of virtual sensors, actuators and a signal processing structure. The signal processing structure controls the adaptive system under changing environmental conditions by generating actuator signals based on sensor signals derived from the environment. The target has been to achieve a system behavior which reduces the airfoil's drag, calculated in a CFD (computational fluid dynamics) simulation of the resulting airfoil shape while maintaining specified lift value. The actuator signals correspond to changes of the NURBS [6] control points and define the current airfoil shape. The virtual sensors of the system have been defined as pressure sensors, at a given position on the airfoil surface. The values of the virtual sensors correspond to the surface pressure calculated in the CFD simulation and therefore depend on the blade's surface, the angle of attack and the speed of the air flow etc. Fig. 1 (a) shows the described relations between the single parts of the test-framework. With the described setup an adaptive behavior can be realized by the actuators in reaction to the change of the environmental conditions. Furthermore a variable number of sensors or actuators can be easily realized. The described setup serves as a test framework for the simulation of the interactions between control structure and morphology during the operation of the control structure as well during their evolutionary development.

In our work we implemented the two dimensional airfoil by a non-uniform rational B-splines (NURBS) as shown in Fig. 1 (b). The shape of the NURBS

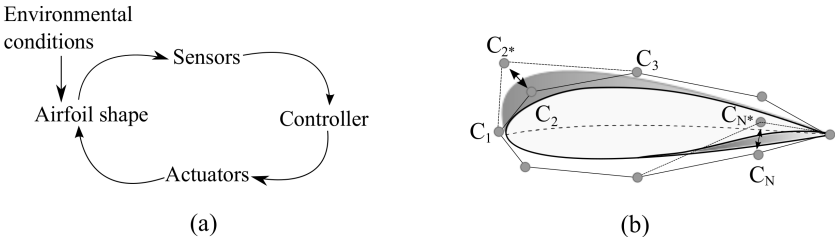

Fig. 1. (a) Adaptive airfoil framework, (b) Example of the airfoil created with NURBS. Airfoil in white, defined by the initial positions of the spline control points. The airfoil shape change (in gray) results from the movements of C_2 and C_N.

curve and with that the shape of the resulting wing profile is determined by the set of spline control points. The splines, defined by its control points C_n, result into a unique two dimensional airfoil shape. By moving the control points in the two dimensional space, a shape change of the airfoil can be achieved. For the simulation of the aerodynamic airfoil characteristics and pressure distribution we used the computational fluid dynamic solver Xfoil[1] because of its high speed which is decisive for optimization tasks (less than 5 seconds). Xfoil calculates different aerodynamic characteristics for the given airfoil geometry and environmental configurations, e.g. angle of attack, Reynolds number etc. In the simulation we change the angle of attack as a variable input of the system in order to generate variations of the airfoil environment. The Reynolds number has been fixed during the optimization($Re = 10^7$). To simulate the sensors we used the distribution of the pressure coefficient over the airfoil surface. The pressure coefficient C_p [7] is defined as a relative pressure throughout a flow field in fluid dynamics. In comparison to a gauge pressure value at the point on the airfoil, the pressure coefficient is dimensionless and independent from effects of the density and speed of the air. We used Xfoil to calculate the profile of the pressure coefficients C_p at 160 points on the airfoil surface. A sensor placed on the airfoil returns a sensor value corresponding to the pressure coefficient at the airfoil surface.

2.1 Controller

The control system is realized by Parker and Nathan [2] as well as Bugajska and Schutz [3] as a reactive system that uses "if...then" rules to control a simulated robot. Haller, Ijspeert and Floreano [8] implemented a controller inspired from the central pattern generators underlying locomotion in animals. In comparison to these approaches we use biologically inspired feed forward neural networks (FFNN). The task of the neural controller is to reduce the drag of the adaptive airfoil system by morphing the airfoil surface. For the implementation the SHARK[2], open-source C++ machine learning library is used. The neural

[1] http://web.mit.edu/drela/Public/web/xfoil/
[2] http://image.diku.dk/shark/

network we implemented consists of one input layer, a single hidden layer with sigmoidal activation function and one output layer with a linear activation function. In Fig. 2 a schematic overview of the overall system is given.

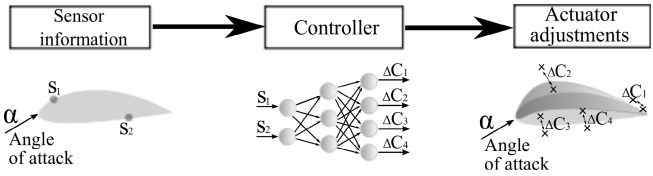

Fig. 2. Schematic view of the overall control structure

3 Baseline Optimization

The target of the baseline optimization has been to find shapes for the airfoils with minimal drag in order to generate a baseline which allows the evaluation of the blade shapes generated by the adaptive system. A second reason for the experiments was to investigate the influence of the number of spline control points on the optimization behavior. To determine the maximal achievable quality of the airfoils conventional evolutionary design optimization was performed. We used a CMA-ES(4,8) strategy with standard population size [9] to find the optimal shapes of the airfoil for the individual angles of attack with lift constraint. Minimal lift constraint has been set to a lift coefficient of NACA 2410 airfoil, $C_l^{min} = C_l^{NACA2410}$. NACA airfoils are the aircraft wing shapes, developed by the National Advisory Committee for Aeronautics in 1948 [10] and define since that time a set of standard airfoil shapes. Fig. 3.a) shows the result of the design optimization with fixed number of spline control points, $C_p = 6$. The maximal thickness of the airfoil was set to the maximal thickness of the NACA 2410 airfoil which is equal to 10% of the chord. For a set of 5 angles of attack the optimal airfoil shapes have been determined experimentally with the resulting drag and lift coefficients given in Table 1. We found specialized solutions for each angle of attack, which have significantly lower drag and higher lift than a single NACA 2410 airfoil being rather robust for wide range of different angles of attack.

The results of the optimization runs can be seen as the maximal achievable performance for the given settings and therefore form the baseline for the evaluation of all further experiments. From here on we concentrate on the sensor-controller optimisation. In a first set of experiments we investigate the influence of the number of spline control points on the optimization results. In the design optimization runs with only 3 variable control points per airfoil we observe a very high improvement of the blade quality in an early phase of the optimization, however with a low final quality. With a higher number of spline control points the airfoil quality improves slower, but the final quality of the airfoil is significantly improved.

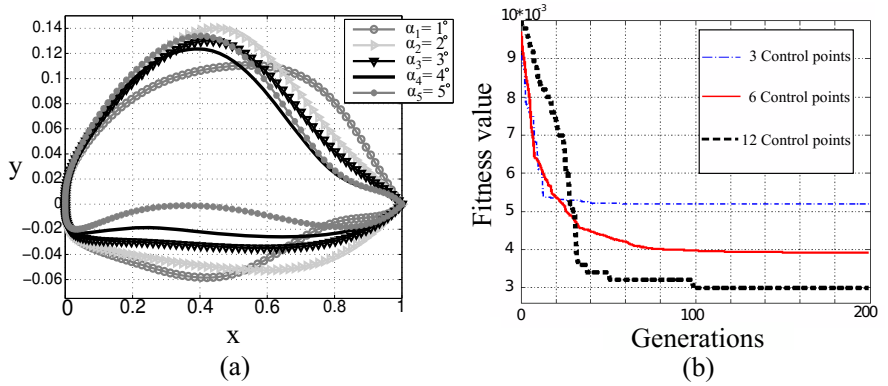

Fig. 3. (a) Optimized airfoil shapes, (b) Averaged quality history of CMA optimisation runs for different number of spline control points. Angle of attack was set to 3°, slightly different start airfoils were used in all 5 of the otherwise identical simulations which were used for averaging.

Table 1. Best baseline performance with 6 spline control points, compared with NACA 2410 airfoil

$\alpha, degree$	$C_d^{opt} 10^{-3}$	C_l^{opt}	$C_d^{NACA2410} 10^{-3}$	$C_l^{NACA2410}$
1°	3.091	0.401	4.950	0.355
2°	3.192	0.497	5.070	0.467
3°	3.391	0.617	5.390	0.576
4°	3.434	0.845	5.910	0.686
5°	3.860	0.931	6.140	0.791

4 Robust Sensor-Controller Optimization

We implemented the optimization of sensor positions on the airfoil surface and the optimization of neural network weights. We realized the proposed optimization task with a standard Evolution Strategy (ES), developed by Bienert, Rechenberg and Schwefel as well as with a CMA Evolution Strategy [11], [9]. We achieved significantly better results with a standard ES(50,200) with two different self adapted step sizes, for sensor positions and neural network weights adaptation. Detailed results are given in section 4.2.

4.1 System Performance Evaluation

The task for the controller is the improve the airfoil drag after a variation of the inflow angle. Therefore the drag coefficient of the airfoil before any modifications took place C_d^1 is evaluated and after the modification of the airfoil blade C_d^2. The ratio of these two values shows if the neural network outputs realizing an actuator adjustment, perform well and reduce the airfoil drag. The total fitness of the individual has been defined as the sum of the drag coefficient value ratios summed

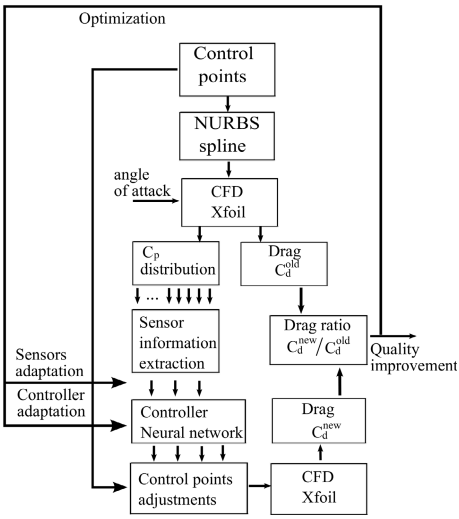

Fig. 4. Overview of the system evaluation

over the set of different angles of attack given in the experimental setup. Fig. 4 shows the structural diagram of individual evaluation. Optimization starts with randomly initiated sensor positions between 0 (trailing edge, wing upper-side) and 2 (trailing edge, wing under-side) and neural network weights, uniformly randomly initialized between -0.01 and 0.01. The trailing edge is defined as rear edge, where the airflow split by the leading edge rejoins [7]. After the change of the angle of attack we evaluated 3 cycles of geometry change in order to let the system convert to a final state. The main reason is that the system goes through a set of partial update steps until the optimal geometry is reached. After the first update the adjusted geometry is therefore likely to be influenced by the shape in the previous step as visible in the final results. The final fitness value for the individual is calculated as the sum of drag value ratios over all tree steps of spline control point adjustments for a single angle of attack and additionally over a cascade of different angles of attack, which however stayed the same during the first experiment. In the second experiment, in each generation a set of angles of attack have been randomly changed between 2° and 4°. The random change was introduced to avoid that only shape transitions which are predefined by the set of given inflow angles are possible. As mentioned, the size of the controller was defined by the number of neurons in the input layer which is equal to the number of sensors, the number of neurons in the output layer equal to the number of actuators and a fixed number of 20 hidden neurons.

4.2 Robust Optimization Results

Fig. 5 shows the filtered fitness curves of the robust optimization described in section 4.1 averaged over 10 runs. The fitness function was defined as following:

$$Fitness(Individual) = \frac{\sum_{\alpha=1}^{N} \sum_{i=1}^{M} \frac{C_d(\alpha,\text{changed airfoil})}{C_d(\alpha,\text{unchanged airfoil})}}{N * M} \quad (1)$$

where M is a number of controller actions for the same angle of attack ($M = 3$) ,α is the angle of attack, N is the total number of angles of attack applied and the individual has been evaluated on, C_d is the drag coefficient. The number of

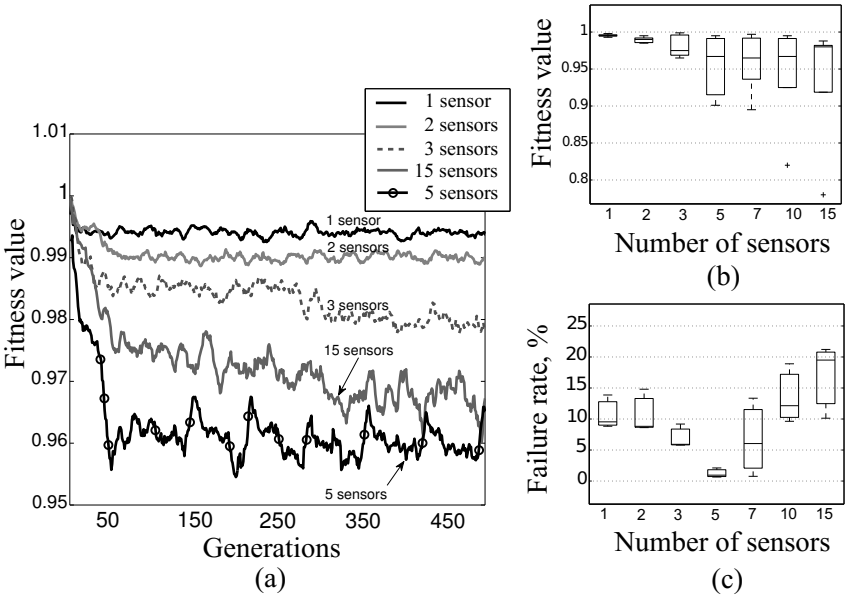

Fig. 5. (a) Robust optimization results filtered with moving average over 10 generations. Fitness curves has been averaged over 10 runs with different starting parameters. (b) Box plot of the optimization runs for each number of sensors, (c) Percentage of the cases in which controller lead to a failure performance, for scenario of 10 random angles of attack between 1° and 7°.

optimization parameters results from the size of system controller (number of neurons in a hidden layer), the number of sensors and actuators (control points of the spline). The total number of parameter is

$$N_{Param} = N_i * N_h + (N_i + N_h) * N_o + N_h + N_o + N_i + N_s \quad (2)$$

where N_i is the number of sensors, N_h the number of neurons in the hidden layer (was fixed to $N_h = 20$), N_o is the number of actuators (was fixed to $N_o = 6$) and N_s is the number of optimization step-sizes ($N_s = 2$). As an example, for the system, using 5 sensors, we need to optimize 283 parameters.

The results show that the system development progress depends on the number of sensors. For the systems, using between 1 and 5 sensors, we observed a

clear trend of averaged performance improvement with an enlargement of the sensory system (see Fig. 5 (a) and (b)). Starting with 7 sensors the averaged performance does not improve. Additionally in Fig.5 (c) we see, that on average the failure of controller actions, defined as an action, that lead to an invalid solution, increases gradually for the systems with more than 5 sensors,although the maximal achievable quality given in Fig. 5 (b) is better with a larger sensor number.

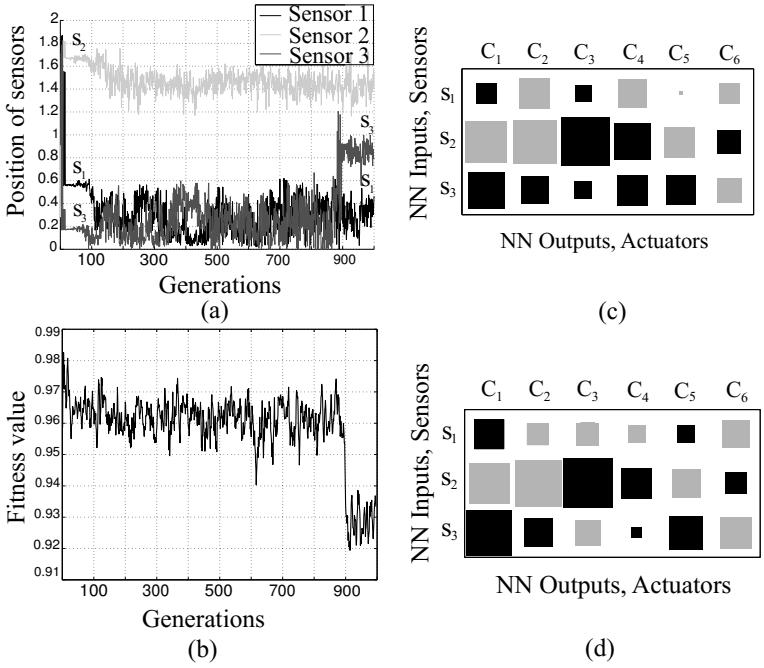

Fig. 6. (a) Development of the position of the sensors during the optimization (b) Optimization of the robust system, using 3 sensors. Evaluation on the random angles of attack between 1° and 5°, Hinton diagrams of the neural controller of the system at generation 800 (c) and 900 (d).

An example of the dynamics of the concurrent sensor-controller adjustment during the optimization experiment is given in Fig. 6. As mentioned, we use single hidden layer, consisting of 20 neurons with sigmoid activation function. To investigate the internal functionality of the neural network as a controller, we visualize converted network connections between sensors and actuators of the adaptive airfoil, omitting the non-linearity of the hidden layer. The connection strengths between neurons have been calculated as following:

$$S_{io} = \frac{\sum_{j=1}^{j=N_h} W_{ij} V_{jo}}{N_h} \tag{3}$$

The variable S_{io} is the converted connection strength between input i and output o, N_h is the number of neurons in a hidden layer, W and V - input and output weights of the neural network. Fig. 6 (c) and (d) show corresponding diagrams of the neural strengths of the system at the 800th and 900th generation. For visualizing of the converted neural connection strengths a Hinton diagrams has been used [12]. The size of the boxes corresponds to the value of the connection strength. The boxes color (gray and black) represents positive or negative sign of the connection strength respectively. The values of the connection strengths lie between zero (no box) and one (box of maximum size). In Fig. 6 (b) we see a significant performance improvement at the generation 900. Fig. 6 (a) shows the development of the sensory system configuration. Sensor 3 changes its position gradually at around the 900th generation. The corresponding change in a controller system can be observed in Fig. 6 (c) and (d). Compared with the controller at generation 800, we can see a significant change of the controller connection strengths at generation 900 for the first and the third sensor. The connections of the second sensor stay nearly constant. Regarding Fig. 6 (a), (b), (c) and (d), a precise sensor-controller adjustment takes place. This results show that the development of the signal measurement and signal processing modules are tightly coupled and precisely coordinated.

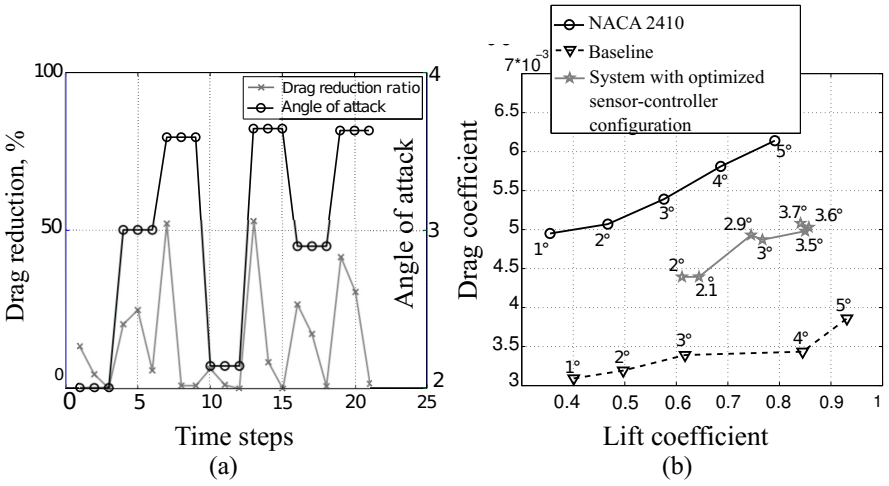

Fig. 7. (a) Percentage of the airfoil drag reduction for a scenario of 7 angles of attack between 2° and 4°, using 7 sensors. (b) Comparison of the robust system performance given in Fig.7 (a) with baseline design optimization in Fig. 3 (a), Tab. 1 and NACA 2410.

Finally we analyzed the results of the robust sensor-controller optimization in Fig. 5. The performance of the optimized system with 7 sensors was again evaluated this time with a set of 7 randomly chosen angles. The result is illustrated in) Fig. 7 (a). As mentioned, the controller adjusts the actuators for the

current angle of attack in 3 steps. We observe the drag reduction after almost each controller action. The highest drag reduction takes place in the first of 3 controller actions for the same angle of attack. For example the drag reduction for the angles of attack of 3.5° and 3.6° was above 50% through the first controller adjustment. The fitness value of the system in Fig. 7 (a) is equal to 0.85. Fig. 7 (b) shows a final comparison of the airfoils resulting from a concurrent sensor-controller development, from the standard design optimization and the NACA 2410 airfoil. We observed, that on the test scenario the system with a concurrently optimized sensor and controller configuration does not perform as well as the individual design optimization with respect to a drag, but performs better than NACA 2410 airfoil. Regarding the lift coefficient, the co-evolved system creates higher lift than the profiles of baseline optimization and NACA 2410 for the same angles of attack.

5 Conclusions

This work investigates the generation of an adaptive system realized by an adaptive wing. The system consists of a sensor and actuator configuration as well as a related control structure. The target for the adaptive wing is the minimization of the airfoil drag while the angle in which the air is approaching the airfoil is changed randomly. Sensors as well as the control structure of the adaptive wing design are defined during an evolutionary process, resulting in a concurrent and coordinated development of the overall system. The experimental results demonstrate the expected high correlation between the development of the sensory system and the control systems. Furthermore we observe a strong influence of the number of the environmental sensors, which is related to the amount of information which is available to the control structure, and the final performance of the system. On the one hand the system needs sufficient sensory information defined by the number and position of the sensors for an optimal control strategy in the randomly changing environment. On the other hand the achieved quality of the optimized solution degenerates with very high numbers of optimization parameters, which are determined by the complexity of the control structure which in turn is defined by the number of sensory inputs. Both aspects can be observed in the experimental results. A small number of sensors results in simple and low dimensional control structures which converge quickly in the evolutionary process to a local optimum, yet they have an overall low quality measured by a high drag value due to insufficient sensory information. In the case of a high dimensional sensory input of the system we observe low convergence speed toward an optimum due to the high dimensional optimization problem or even an early convergence to local optima. These results suggest the existence of an optimal number of system parameters for the evolutionary design process. Unfortunately neither the optimal dimensionality of the sensory input nor the optimal number of optimization parameter is known for the problem at hand. Furthermore it is likely that the optimal number of parameters depend on the progress of the optimization process. These findings suggest the necessity of a variable

number of free parameters in the system, which is addressed in future work by the realization of a growth process during the evolutionary design process.

Acknowledgments. The authors gratefully acknowledge the support of Giles Endicott and Bernhard Sendhoff and the financial support from Honda Research Institute Europe GmbH.

References

1. Sims, K.: Evolving virtual creatures. In: The 21st Annual Conference, pp. 15–22. ACM Press, New York (1994)
2. Parker, G., Nathan, P.: Co-evolution of sensor morphology and control on a simulated legged robot. In: International Symposium on Computational Intelligence in Robotics and Automation, CIRA 2007, pp. 516–521 (2007)
3. Bugajska, M.D., Schultz, A.C.: Coevolution of form and function in the design of micro air vehicles. In: Evolvable Hardware, 154–166. IEEE Computer Society (2002)
4. Sugiura, K., Akahane, M., Shiose, T., Shimohara, K., Katai, O.: Exploiting interaction between sensory morphology and learning. In: 2005 IEEE International Conference on Systems, Man and Cybernetics, vol. 1., pp. 883–888 (2005)
5. Auerbach, J., Bongard, J.: 12th International Conference on the Synthesis and Simulation of Living Systems (ALife XII) (August 2010)
6. Farin, G.E.: NURBS: From Projective Geometry to Practical Use, 2nd edn. A. K. Peters Ltd., Natick (1999)
7. Anderson, J.: Fundamentals of Aerodynamics. Anderson series, McGraw-Hill Education (2011)
8. von Haller, B., Ijspeert, A.J., Floreano, D.: Co-evolution of Structures and Controllers for Neubot Underwater Modular Robots. In: Capcarrère, M.S., Freitas, A.A., Bentley, P.J., Johnson, C.G., Timmis, J. (eds.) ECAL 2005. LNCS (LNAI), vol. 3630, pp. 189–199. Springer, Heidelberg (2005)
9. Hansen, N.: The CMA Evolution Strategy: A Comparing Review (2006)
10. Jacobs, E.N., Ward, K.E., Pinkerton, R.M.: The characteristics of 78 related airfoil sections from tests in the variable density wind tunnel. Technical Report 460 (1948)
11. Rechenberg, I.: Evolutionsstrategie 1994. Frommann, Stuttgart (1994) Fit via Evolutionsstrategie, Routine von Volker Tuerck vorhanden (1994)
12. Bremner, F., Gotts, S., Denham, D.: Hinton diagrams: Viewing connection strengths in neural networks, vol. 26, pp. 215–218. Springer (1994)